

Retardation effects in radiative electron capture

M. C. Pacher, A. D. González, and J. E. Miraglia

*Instituto de Astronomía y Física del Espacio, Consejo Nacional de Investigaciones Científicas y Técnicas,
Casilla de Correo 67, Sucursal 28, Buenos Aires 1428, Argentina*

(Received 12 September 1986)

Three-particle radiative electron-capture cross sections with retardation are calculated within the nonrelativistic treatment. The formalism is carried out in the laboratory frame. It is found that the center of mass genuinely radiates, and it plays an important role in restoring the backward-forward symmetry for angular distributions. Comparison with experiments are made. The formalism also describes the nonrelativistic Doppler effect which shifts and spreads the photon energy distributions. Total, single-, and double-differential cross sections are reported, and comparisons with the dipole approximation are presented. The range of validity of the results obtained is discussed.

I. INTRODUCTION

Single radiative electron capture (REC) is a collision process in which an impinging projectile captures an electron from a given target atom, and a photon is emitted. Here we shall *differentiate* it from recombination, where the electron is initially free. In REC at least three particles are involved [namely, projectile (P), target (T), and electron (e)], while in recombination only two particles play a role (say, P and e). The two processes are closely related.

Single-differential and total cross sections were reported by using several approximations.¹⁻⁵ In most of the cases the dipole approximation was assumed, which consists of considering that the emitted photon has energy but not momentum. This assumption is fully justified for small impact velocities, but not for large ones. For example, for REC proton-hydrogen collisions, the relevant photon energies ω are found to be around $v_i^2/2$, where v_i is the ion velocity, and the photon momentum is $k = \omega/c = 0.5v_i^2/c$. Therefore, for impinging velocities larger than 17 (that is 7 MeV/amu), we have $k > 1$, and the photon momentum should not be neglected. Atomic units are used except where otherwise indicated.

The dipole approximation leads to the well-known photon angular distribution: $A + B \sin^2\theta$, where θ is the photon angle with respect to the incident beam. For recombination $A = 0$ (Ref. 6), while for REC $A \rightarrow 0$ as $v_i \rightarrow \infty$. When $v_i/c \ll 1$, such an angular distribution holds in the center of mass as well as in the laboratory frame, giving rise to a forward-backward symmetry.

As the impinging velocity increases, three kinds of effects come into existence, namely, aberration,⁷ Doppler effect,⁷ and retardation.⁶ The first one arises from the Lorentz transformation of angles from the center of mass to the laboratory frame, the second one from the corresponding transformation of photon energies, and the third one considers the photon momentum.

If the calculation is carried out in the center of mass with the dipole approximation, the aberration shifts the

distribution to the forward direction in the laboratory frame. Some experimental evidence seemed to agree with such a shape⁸ (in contrast with a previous work⁹). In a subsequent paper Spindler *et al.*¹⁰ noted that retardation effects (which are known to provide backward distributions in the center of mass) cancel the Lorentz transformation to restore the $\sin^2\theta$ behavior in the laboratory frame. The experiments were found to exhibit forward-backward symmetry,¹⁰ in agreement with their theoretical predictions. More recently, Anholt *et al.*¹¹ have found experimental evidence of symmetry even at relativistic velocities and high Z_P ions. They have also shown theoretical calculations¹² using a relativistic approach, which agree with the data to within 6%.

In our opinion the models used so far were constructed with different corrections, and they are not derived from a formal and unique approach as one would like. In the present work we present a rigorous formalism to treat both recombination and REC processes within the nonrelativistic approximation, considering *only* the photon momentum.

In Sec. II we shall begin analyzing the recombination process, where the method outlined by Shakeshaft and Spruch¹³ will be followed. We briefly discuss some aspects of formal theory. We want to remark here that the nonrelativistic Doppler effect is naturally attained after integrating on the final density of states, including the center of mass. Angular distributions and total cross sections are calculated, and comparisons with the dipole approximation are made. As we shall see, when retardation effects are taken into account, the center of mass *can genuinely radiate*. It plays an important role at the level of differential cross sections restoring the $\sin^2\theta$ -type behavior, for $v_i/c < 0.5$, in the frame where the electron is at rest. Comparisons with experimental data are presented.

In Sec. III we analyze the three-particle REC with the same criteria. A formalism recently developed by ourselves¹⁴ is followed. The problem is more difficult to handle, due to the additional projectile angular distribution,

not present in recombination. In order to make the corresponding calculations, we have resorted to the exact impulse approximation wave function to describe the initial state, and the unperturbed wave function one as the final state. The reason for this is twofold. First, these wave functions are off-shell orthogonal, and this condition is necessary to avoid spurious radiation of the center of mass in the dipole limit.¹⁴ And second, the impulse approximation contains the P - e continuum state which fully describes the recombination.

In Sec. IV we present REC results with retardation for proton-hydrogen collisions. Energy distributions and total cross sections are presented. We find the recombination model gives a good account of REC, at the level of angular distributions, for high impinging velocities. At the level of energy distributions we find dramatic changes when compared with the dipole approximation, due mainly to the Doppler effect. At very high projectile velocities, retardation effects introduce small corrections to the total cross section, giving rise to an unexpected difference between REC and recombination models.

II. RECOMBINATION: TWO-PARTICLE MODEL

REC can be regarded, at high projectile velocities, as a binary e - P radiative recombination, independent of the nucleus target. The present section deals with recombination with retardation. In order to make a direct comparison with REC experiments (where the target atom is at rest), we shall consider the electron at rest in the laboratory frame, and the projectile coming in. The process, as well as the radiating field, will be described in the laboratory frame.

A. Shakeshaft-Spruch model

The matter-radiation interaction for spontaneous emission is given by¹³

$$\mathcal{H}_I = iA_0 \hat{\lambda}_I \cdot \exp(-i\mathbf{k} \cdot \mathbf{X})(B \nabla_x + b \nabla_r), \quad (2.1)$$

where $A_0 = 1/(2\pi\sqrt{\omega})$, $\hat{\lambda}_I$ is the unit polarization vector, \mathbf{X} is the center-of-mass coordinate, \mathbf{r} is the relative coordinate,

$$B = [Z_P \exp(i\mathbf{k} \cdot \mathbf{r}/M_2) - \exp(-i\mathbf{k} \cdot \mathbf{r}M_P/M_2)]/M_2, \quad (2.2)$$

$$b = -(Z_P/M_P)[\exp(i\mathbf{k} \cdot \mathbf{r}/M_2) - \exp(-i\mathbf{k} \cdot \mathbf{r}M_P/M_2)], \quad (2.3)$$

Z_j and M_j are the charge and mass of the particle j ($j = P, T, e$), and M_2 is the total mass of the two interacting particles: $M_2 = M_P + 1$.

The matrix element of the matter-radiation interaction reads

$$\langle \mathcal{H}_I \rangle_{fi} = \delta(\mathbf{U}_i - \mathbf{U}_f - \mathbf{k}) \langle H_I \rangle_{fi}, \quad (2.4)$$

where \mathbf{U}_i and \mathbf{U}_f are initial and final moments of the center of mass,

$$\langle H_I \rangle_{fi} = {}^2H_I^{c.m.} + {}^2H_I^E, \quad (2.5)$$

$${}^2H_I^{c.m.} = A_0 \hat{\lambda}_I \cdot (\mathbf{U}_i/M_2) \langle \varphi_f | \exp(-i\mathbf{k} \cdot \mathbf{r}) | \varphi_i \rangle, \quad (2.6)$$

$${}^2H_I^E = -iA_0 \hat{\lambda}_I \cdot \langle \varphi_f | \exp(-i\mathbf{k} \cdot \mathbf{r}) \nabla_r | \varphi_i \rangle. \quad (2.7)$$

To derive these expressions, we have used the orthogonality property of the quantum electron states, i.e., $\langle \varphi_f | \varphi_i \rangle = 0$, and considered a heavy impinging projectile, i.e., $M_{P,T} \gg M_e = 1$.

In the dipole approximation $k = 0$, the center of mass does *not* recoil, and therefore it cannot radiate. This can be seen from Eq. (2.6) since φ_f and φ_i are orthogonal, and so ${}^2H_I^{c.m.} = 0$ (Ref. 13). When retardation effects are included, the center of mass *does* recoil, to take into account the photon momentum, and so ${}^2H_I^{c.m.} \neq 0$. The larger the projectile velocity is, the larger k is, and then the more relevant such a term will be. We anticipate that it plays an important role in the high-velocity limit. ${}^2H_I^{c.m.}$ depends on

$$(\mathbf{U}_i/M_2) = \mathbf{v}_{c.m.}, \quad (2.8)$$

$\mathbf{v}_{c.m.}$ being the velocity of the center of mass with respect to the observer. In particular, if the observer were in the center-of-mass system (i.e. on the projectile due to the fact that it is heavy), this term is null. As mentioned before, we described the collision in the laboratory frame; then $\mathbf{v}_{c.m.} = \mathbf{v}_i$, where \mathbf{v}_i is the projectile velocity.

In particular for recombination, we have

$$\varphi_i(\mathbf{r}) = \psi^+(Z_P, -\mathbf{v} | \mathbf{r}), \quad (2.9)$$

where $\psi^+(Z, \mathbf{v})$ is the continuum state of the electron in the field of a Coulomb charge Z , with velocity \mathbf{v} , and φ_f is the final bound state. In the present calculation we have considered just the $1s$ ground state. Using Eq. (2.9) in Eqs. (2.6) and (2.7), we obtain Nordsieck-type integrals, which can be expressed in closed form. The same view point makes a simple extension of Eqs. (2.4)–(2.7) to bremsstrahlung and photoelectric processes possible.

B. Comments on the formal theory

The probability of transition per unit time is here given by

$$\frac{dw}{dt} = 2\pi \delta(E_i - E_f) \delta^2(\mathbf{U}_i - \mathbf{U}_f - \mathbf{k}) \sum_{l=1}^2 |\langle H_l \rangle_{fi}|^2 d\mathbf{U}_f d\mathbf{k}, \quad (2.10)$$

where

$$E_i = \frac{U_i^2}{2M_2} + \frac{v_i^2}{2}, \quad E_f = \frac{U_f^2}{2M_2} + \varepsilon_f + \omega. \quad (2.11)$$

The relation between $\langle \mathcal{H}_I \rangle_{fi}$ and $\langle H_I \rangle_{fi}$ in Eq. (2.4) is similar to the one between the transition matrix and its reduced form (see, for example, Ref. 15 or 16). Therefore the handling of the δ^2 in Eq. (2.10) follows the same treatment as in the formal theory of scattering. First, the use of wave packets removes one $\delta(\mathbf{U}_i - \mathbf{U}_f - \mathbf{k})$ after integrating over the corresponding amplitudes.¹⁷ Dividing by the relative flux, and integrating on the final density of

states, we find that the differential cross section is given by

$$\frac{d\sigma_2}{d\Omega} = \frac{(2\pi)^4}{c^3 v_i} \int_0^\infty d\omega \omega^2 d\mathbf{U}_f \delta(E_i - E_f) \delta(\mathbf{U}_i - \mathbf{U}_f - \mathbf{k}) \times \sum_{l=1}^2 |\langle H_l \rangle_{fi}|^2 \quad (2.12)$$

$$= \frac{(2\pi)^4}{c^3 v_i |1 - \beta \cos\theta|} \int_0^\infty d\omega \omega^2 \delta(\omega - \omega_{L2}) \times \sum_{l=1}^2 |\langle H_l \rangle_{fi}|^2, \quad (2.13)$$

where

$$\omega_{L2} = \frac{v_i^2/2 - \varepsilon_f}{1 - \beta \cos\theta}, \quad (2.14)$$

$\beta = v_i/c$, and ε_f is the final binding energy. To derive Eq. (2.14) we have neglected terms of order k^2/M_2 . By integrating Eq. (2.13) we finally arrive at

$$\frac{d\sigma_2}{d\Omega} = \frac{(2\pi)^4}{c^3 v_i} \frac{\omega_{L2}^2}{(1 - \beta \cos\theta)} \sum_{l=1}^2 |{}^2H_l^{c.m.} + {}^2H_l^E|^2, \quad (2.15)$$

where all the quantities are now evaluated on the energy and momentum shell, i.e., with ω_{L2} and $k = \omega_{L2}/c$.

C. Discussions and results

To deal with the calculation of photon distributions, we have two alternatives: either the usual one¹⁰—to perform the calculation in the center of mass frame and then to transform to the laboratory frame by imposing aberration and the Doppler shift; or, as in our case, to directly perform the calculation in the laboratory frame. In this case the *only* use of retardation induces the radiation of the center of mass, and the correction to the photon energy, Eq. (2.14), can be certainly understood as the Doppler correction of the first alternative. Both ways should be equivalent to order β , but *not* to β^2 and higher order.¹³

Photon angular distributions for the simple collision $H^+ + e \rightarrow H(1s) + \omega$ are displayed in Fig. 1 for four impinging velocities. Up to velocities as large as 60 (near 100-MeV protons), the shapes are very closed to $\sin^2\theta$. The single results are also plotted in dashed and dotted lines, denoted with EB (electron bremsstrahlung) and CMB (center-of-mass bremsstrahlung), respectively. Note the EB term alone tends, as $v \rightarrow \infty$, to give a backward distribution, while the CMB interferes to restore a backward-forward symmetry. The range of validity of our nonrelativistic theory would be established for, say, $v_i < c/2 = 68$.⁴ In all this range, distributions peak very near 90° s. At $v_i = 90$, well out of the range of validity of nonrelativistic theory, the results present two separate peaks. We have calculated forward-backward ratios for sulfur and oxygen ions impinging on stationary electrons, and the ratios agree with the measurements within the experimental errors (see Table 1 Ref. 10).

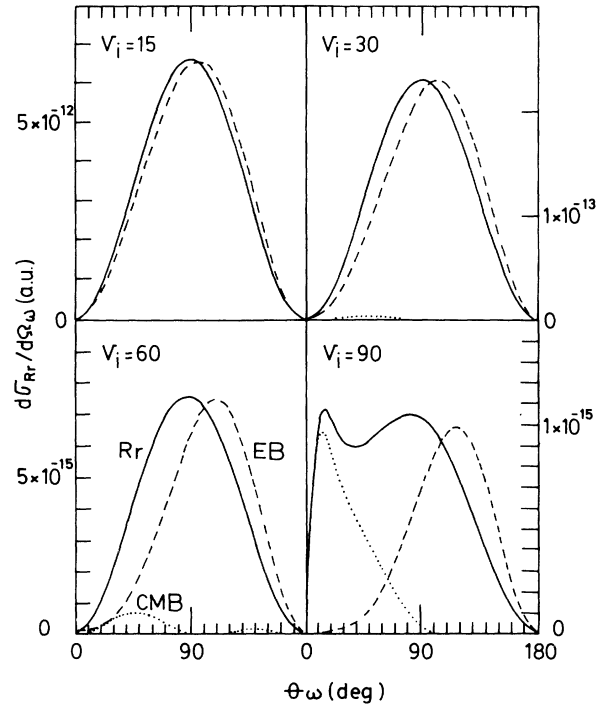
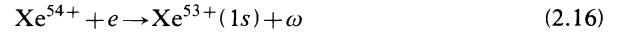


FIG. 1. Photon angular distributions for the recombination $H^+ + e \rightarrow H(1s) + \omega$ for four impinging proton velocities. Cross sections are calculated in the laboratory frame where the electron is initially at rest. Notation: θ_ω is the angle of emission of the photon, Rr represents recombination with retardation, EB and CMB represent the electron and center-of-mass bremsstrahlung partial results, respectively [see Eq. (2.5)]. Note the nonrelativistic formalism is not valid for $v_i = 90$.

In order to test our model to the limit, we have calculated the process



at 197 MeV/u. The impinging velocity is 77 [$\gamma = 1/(1 - \beta^2)^{1/2} = 1.2$], and therefore the nonrelativistic theory is rather out of the range of validity (also the Xe charge is high and the electron wave function should be described by a proper relativistic treatment). Calculations are shown in Fig. 2 and compared with the experiments of capture from beryllium. Results were normalized to the data, and this factor is related to vacancy number.¹¹ Our theoretical results peak at 85° , and account for the shape quite well. Here the term ${}^2H_l^{c.m.}$ is very relevant to restoring the $\sin^2\theta$ -type shape, since the term ${}^2H_l^E$ alone peaks at 115° .

Figure 3 displays ratios of total cross sections to the recombination with the dipole approximation. Note the departure from the well-known v_i^{-5} behavior. That overestimation is due to the CMB, which is the dominant term in the limit.

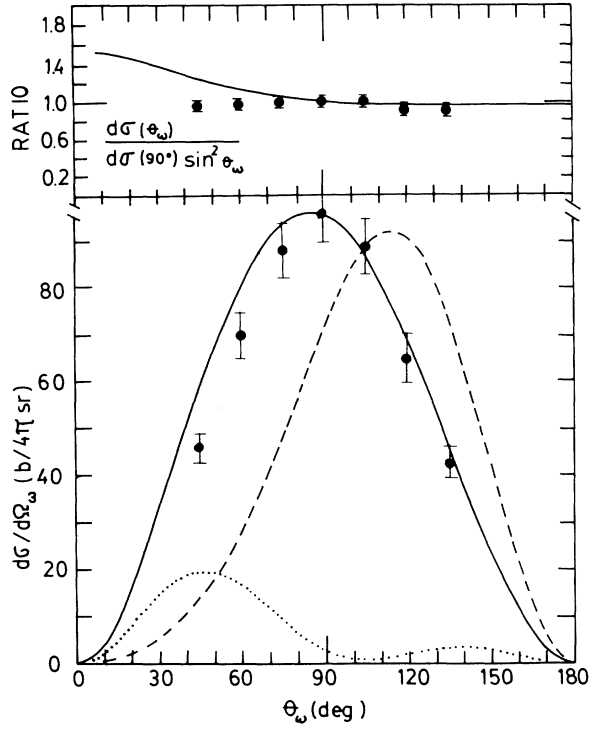


FIG. 2. Photon angular distribution for the recombination $\text{Xe}^{54+} + e \rightarrow \text{Xe}^{53+}(1s) + \omega$ calculated in the center of mass where the electron is initially at rest. The colliding velocity is 77 (in atomic units). Theory as in Fig. 1, and experiments from Anholt *et al.* (Ref. 11) corresponding to Xe (197 MeV/u) impinging on beryllium.

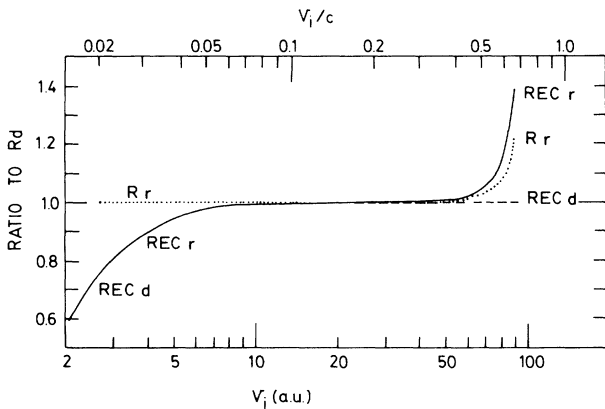


FIG. 3. Ratios of total cross sections to recombination with dipole approximation (Rd) for $\text{H}^+ + e \rightarrow \text{H}(1s) + \omega$ as a function of the proton velocity. Results were carried out in the laboratory frame where the electron is initially at rest. Notation: Rr represents recombination for $\text{H}^+ - e$ with retardation, RECd represents radiative electron capture $\text{H}^+ + \text{H}(1s) \rightarrow \text{H}(1s) + \text{H}^+ + \omega$ with the dipole approximation, REC r represents radiative electron capture as before with retardation.

III. RADIATIVE ELECTRON CAPTURE: THREE-PARTICLE MODEL

The extension to the three-particle system of the Shakeshaft and Spruch model has been derived in Sec. 2 of Ref. 14. Wave functions for such systems are not exactly known, and here we shall resort to the exact impulse approximation to describe the initial channel [see Eq. (A2) Ref. 14] and the nonperturbed for the final one [see Eq. (A3) of Ref. 14]. The wave functions are off-shell orthogonal as the exact ones are, and so no spurious radiation is expected in the dipole approximation limit.

When k is retained and $M_{T,P} \gg 1$, we have obtained after algebra similar to that of Sec. II, the following expression for the fivefold differential cross section:

$$\frac{d\sigma_3}{d\Omega d\omega d\Omega'} = (2\pi)^4 \frac{v^2}{c^3} \sum_{l=1}^2 |{}^3H_l^{c.m.} + {}^3H_l^{IS} + {}^3H_l^E|^2, \quad (3.1)$$

where $d\Omega'$ is the differential solid angle of the projectile, v_3 is the ion-target reduced mass. $M_3 = M_T + M_P + 1$,

$$H_l^{c.m.} = A_0 \hat{\lambda}_l \cdot (\mathbf{U}_i / M_3) \frac{\tilde{\varphi}_i(\mathbf{W}'_T)}{(2\pi)^{3/2}} \times \langle \varphi_f | \exp(-i\mathbf{k} \cdot \mathbf{r}) | \psi^+(Z_P, \mathbf{W}'_P) \rangle, \quad (3.2)$$

$${}^3H_l^{IS} = A_0 \hat{\lambda}_l \cdot (\mathbf{K}_i / M_P) \frac{\tilde{\varphi}_i(\mathbf{W}'_T)}{(2\pi)^{3/2}} \times \langle \varphi_f | \exp(-i\mathbf{k} \cdot \mathbf{r}) | \psi^+(Z_P, \mathbf{W}'_P) \rangle, \quad (3.3)$$

$${}^3H_l^E = -i A_0 \hat{\lambda}_l \cdot \frac{\tilde{\varphi}_i(\mathbf{W}'_T)}{(2\pi)^{3/2}} \times \langle \varphi_f | \exp(-i\mathbf{k} \cdot \mathbf{r}) \nabla_r | \psi^+(Z_P, \mathbf{W}'_P) \rangle, \quad (3.4)$$

where $\tilde{\varphi}_i$ is the Fourier transform of the initial electronic state on the target, φ_f is the final state on the projectile, and the momentum transfers are given by

$$\mathbf{W}'_T = \mathbf{W}_T + (M_T / M_3) \mathbf{k}, \quad \mathbf{W}'_P = \mathbf{W}_P - (M_T / M_3) \mathbf{k}, \quad (3.5)$$

$$\mathbf{W}_T = \mathbf{K}_i - \mu_T \mathbf{K}_f, \quad \mathbf{W}_P = \mathbf{K}_f - \mu_P \mathbf{K}_i, \quad (3.6)$$

satisfying

$$\mathbf{W}'_T + \mathbf{W}'_P = \mathbf{W}_T + \mathbf{W}_P = \mathbf{v}_i, \quad (3.7)$$

where \mathbf{K}_i is the initial momentum of the projectile, \mathbf{K}_f is the momentum of the final atom with respect to the residual target, and μ_P and μ_T are the (P - e) and the (T - e) reduced masses. From energy and momentum conservation, the components of \mathbf{W}'_T are found to be

$$W'_{Tx} = K_i \sin\theta' \cos\varphi' + (M_T / M_3) k \sin\theta, \quad (3.8)$$

$$W'_{Ty} = K_i \sin\theta' \sin\varphi', \quad (3.9)$$

$$W'_{Tz} = \mathbf{W}'_T \cdot \hat{\mathbf{v}}_i = -\frac{1 - \beta \cos\theta}{v_i} (\omega - \omega_{L3}), \quad (3.10)$$

$$\omega_{L3} = \frac{v_i^2/2 - \varepsilon_f + \varepsilon_i}{(1 - \beta \cos\theta)}, \quad (3.11)$$

where ε_i is the binding energy of the initial electronic state, and φ' denotes the polar and azimuthal angles of \mathbf{K}_f with respect to the plane formed by the ion velocity and the photon momentum. From the previous equations we obtain the dipole approximation by setting $k=0$ and consequently $\beta=0$. Equations (3.2)–(3.4) can be put in closed form by using the Nordsieck technique.

One important point is that now we have three terms instead of two as in recombination [compare Eq. (3.1) with (2.15)]. The third term, Eq. (3.4), clearly involves the electron bremsstrahlung, and the other two inherit the center-of-mass term of the two-particle system in proportions depending on the masses.

Three-particle REC has been considered as a binary P - e recombination weighted with the corresponding Compton profile (see, for example, Ref. 18). After some algebra here we have found the equivalent relation is

$$\frac{d\sigma_3}{d\Omega d\omega d\Omega'} = \frac{K_i^2(1 - \beta \cos\theta)}{v_i} \frac{|\tilde{\varphi}_i(\mathbf{W}'_T)|^2}{(2\pi)^3} \frac{d\sigma_2(\mathbf{v}_i - \mathbf{W}'_T)}{d\Omega}. \quad (3.12)$$

$\mathbf{v}_i - \mathbf{W}'_T$ now replaces the e - P relative velocity. Equation (3.12) presents a peak around $\mathbf{W}'_T=0$ and shaped by $\tilde{\varphi}_i(\mathbf{W}'_T)$. When integrated on $d\Omega'$, the photon energy spectrum is found to be a profile placed when $W'_{Tz}=0$, i.e., around $\omega = \omega_{L3}$ [Eq. (3.11)], differing from two-particle position ω_{L2} [Eq. (2.14)] in the initial binding energy.

We want to mention that Eq. (3.12) is a consequence of the wave function used. For example, if unperturbed wave functions were used, the first-order Born approximation to $d\sigma_2/d\Omega$ would be obtained instead. Further, if the internuclear interaction is considered, a simple expression in terms of recombination is *no longer* possible.

Finally we discuss the equivalence of REC and recombination total cross sections with retardation. From Eq. (3.12) the photon angular distribution is found to be

$$\frac{d\sigma_3}{d\Omega} = \int \frac{d\mathbf{W}'_T}{(2\pi)^3} |\tilde{\varphi}_i(\mathbf{W}'_T)|^2 \frac{d\sigma_2(\mathbf{v}_i - \mathbf{W}'_T)}{d\Omega}. \quad (3.13)$$

As v_i increases, the next steps to follow would be factorizing out the recombination differential cross section (evaluated at v), and integrating the Compton profile. If this is possible, that equivalence would be achieved. Such steps are valid within the dipole approximation *but not* when retardation effects are retained. We anticipate that REC and recombination total cross sections are not equal for $v_i > c/2$ because of the photon momentum.

IV. RESULTS

Four-dimensional integrals were numerically performed to obtain total cross sections, i.e., on φ' , θ' , ω , and θ . Approximately 2.5×10^5 pivots were used, and the total calculation took few hours on our PDP 11/44 minicomputer.

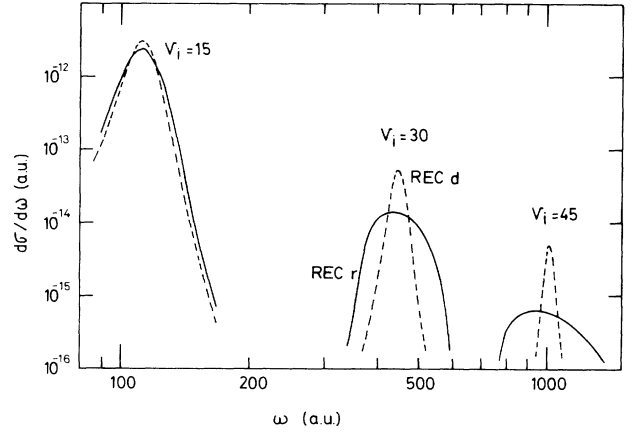
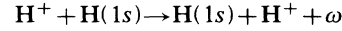


FIG. 4. Single-differential cross sections for $\text{H}^+ + \text{H}(1s) \rightarrow \text{H}(1s) + \text{H}^+ + \omega$ for three impinging velocities as a function of the photon energy. Notation as in Fig. 2.

We have faced this task to find out the changes to the dipole approximation introduced by retardation effects.

REC cross sections with retardation for the process



are displayed in Figs. 3–5. The notation follows this pa-

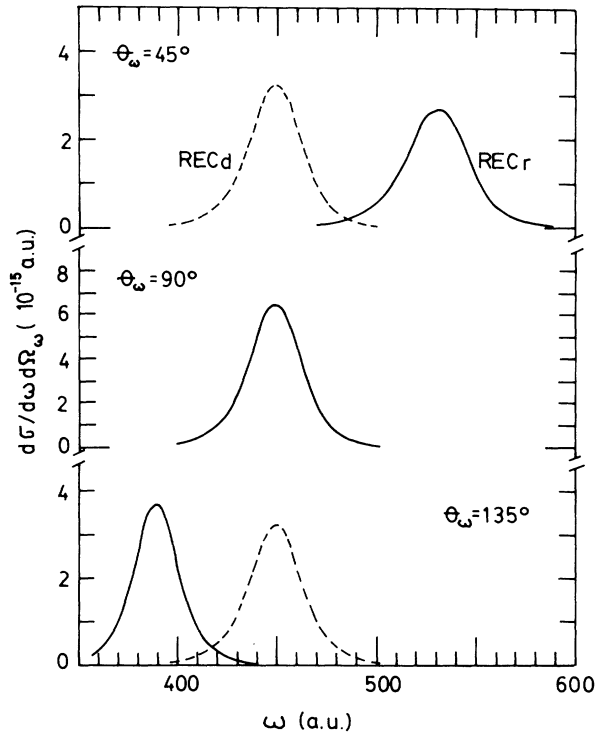


FIG. 5. Double-differential cross sections for $\text{H}^+ + \text{H}(1s) \rightarrow \text{H}(1s) + \text{H}^+ + \omega$ for three different photon angles to the beam, as a function of the photon energy. The proton velocity is 30 in atomic units. Notation as in Fig. 2. At 90° , RECd coincides with RECr.

per; capital letters R and REC denote recombination and radiative electron capture, while the small ones d and r denote dipole approximation and retardation, respectively.

Total cross sections are shown in Fig. 3. Of course, at small velocities REC largely differs from recombination, but in this case retardation corrections are not needed. Up to velocities near $c/2$, REC results are very close to recombination. However for $v_i > c/2$, it is interesting to note the increasing difference between them. Such a difference can be adjudicated to the transverse momenta of the initial electronic distribution occurring in REC but not in recombination. One question now arises: does the equivalence, at the level of total cross section, of recombination and REC processes hold within a proper relativistic calculation for $v_i \rightarrow c$?

In general, retardation introduces meaningful corrections to differential cross sections since it gives terms linear in β . But for total cross sections the linear terms vanish in the corresponding integrations and the retardation leaves only a correction of order β^2 (see Ref. 6, p. 311). As indicated by Shakeshaft and Spruch,¹³ the total cross section is Galilean invariant *only* to order β , therefore corrections of order β^2 introduced by the retardation are *inconsistent* with a proper relativistic calculation.

Photon angular distributions for REC were found to be similar to the ones of recombination shown in Fig. 1.

Small deviations are found at very small and very large angles which make the difference of total cross sections at very high projectile velocities (see Fig. 3).

Photon energy distributions are shown in Fig. 4 for three different proton velocities. Retardation introduces dramatic changes in energy distributions, spilling the well-pronounced peak given by the dipole approximation. Note that the integrated values are the same, since there is not an appreciable difference for total cross sections.

This fact can be explained in terms of the Doppler effect, as shown in Fig. 5. It shows double-differential cross sections for three photon angles at $v_i = 30$. Here we can see the Doppler shift is much larger than the "normal" width. In this way the spreading seen in Fig. 4 can be mainly attributed to Doppler broadening. Coincidentally, at 90° to the beam where most of the experimental energy distributions are carried out, retardation effects vanish. When considering other photon angles, one finds not only that shift but a substantial change of the shape of the profile. For example, in our case, the width of the peak for 45° is 40% larger than the one for 135° . The larger v_i is, the more noticeable this phenomenon becomes. On the other hand, as the target nucleus charge increases, the "natural" width also increases to the point of overtaking the Doppler one.

¹J. S. Briggs and K. Dettmann, Phys. Rev. Lett. **33**, 1123 (1974); J. Phys. B **10**, 1113 (1977).

²M. Gorriz, J. S. Briggs, and S. Alston, J. Phys. B **16**, L665 (1983).

³D. H. Jakubassa-Amundsen, R. Hoppler, and H. D. Betz, J. Phys. B **17**, 3943 (1984).

⁴A. D. González and J. E. Miraglia, Phys. Rev. A **30**, 2292 (1984).

⁵J. E. Miraglia, Phys. Rev. A **32**, 2702 (1985).

⁶H. A. Bethe and E. E. Salpeter, *Quantum Mechanics of One and Two Electron Atoms* (Springer-Verlag, Berlin, 1957).

⁷W. Heitler, *The Quantum Theory of Radiation*, 3rd ed. (Oxford University Press, London, 1954), p. 59.

⁸R. Shule, H. Schmidt-Böcking, and I. Tserruya, J. Phys. B **10**, 889 (1977).

⁹H. D. Betz, F. Bell, H. Panke, and G. Kalkoffen, *Proceedings of the Fourth International Conference on Atomic Physics, Abstracts of Contributed Papers, Heidelberg, Germany, 1974*, edited by J. Kowalski and H. G. Weber (Heidelberg University Press, Heidelberg, Germany, 1974), p. 670.

¹⁰E. Spindler, H. D. Betz, and F. Bell, Phys. Rev. Lett. **42**, 832 (1979).

¹¹R. Anholt, S. A. Andriamonje, E. Morenzoni, Ch. Stoller, J. D. Molitoris, W. E. Meyerhof, H. Bowman, J. S. Xu, J. O. Rasmussen, and D. H. H. Hoffmann, Phys. Rev. Lett. **53**, 234 (1984).

¹²F. Sauter, Ann. Phys. (Leipzig) **9**, 217 (1931); **11**, 454 (1931).

¹³R. Shakeshaft and L. Spruch, Phys. Rev. Lett. **38**, 175 (1977).

¹⁴A. D. González, J. E. Miraglia, and C. R. Garibotti, Phys. Rev. A **34**, 2834 (1986).

¹⁵M. L. Goldberger and K. M. Watson, *Collision Theory* (Wiley, New York, 1964), p. 79.

¹⁶C. J. Joachain, *Quantum Collision Theory* (North-Holland, Amsterdam, 1975), Vol. 2, p. 378.

¹⁷See, for example, Ref. 15, Chap. 3.

¹⁸P. Keinle, M. Kleber, B. Povh, R. M. Diamond, F. S. Stephens, E. Grosse, M. R. Mainer, and D. Proetel, Phys. Rev. Lett. **31**, 1099 (1973).